Coincidence detection of broadband signals by networks of the planned interferometric gravitational wave detectors

Biplab Bhawal and S.V. Dhurandhar
Inter University Centre for Astronomy and Astrophysics, Post Bag 4, Ganeshkhind, Pune-411007, INDIA.
E-mail : biplab@iucaa.ernet.in, sdh@iucaa.ernet.in
(February 7, 2008)

We describe how the six planned detectors (2 LIGOs, VIRGO, GEO, AIGO, TAMA) can be used to perform coincidence experiments for the detection of broadband signals coming from either coalescing compact binaries or burst sources. We first make comparisons of the achievable sensitivities of these detectors under different optical configurations and find that a meaningful coincidence experiment for the detection of coalescing binary signals can only be performed by a network where the LIGOs and VIRGO are operated in power recycling mode and other medium scale detectors are operated in dual recycling mode with a narrower bandwidth. For the model of burst waveform considered by us (i.e. uniform power spectral density upto 2000Hz), we find that the relative sensitivity of the power-recycled VIRGO is quite high as compared to others with their present design parameters and thus coincidence experiment performed by including VIRGO in the network would not be a meaningful one. We also calculate the time-delay window sizes by effectively optimizing the values for different possible networks. The effect of filtering on the calculation of thresholds has also been discussed. We then set the thresholds for different detectors and find out the volume of sky that can be covered by different possible networks and the corresponding rate of detection of coalescing binaries in the beginning of the next century. We note that a coincidence experiment of power-recycled LIGO detectors and VIRGO and dual-recycled GEO and AIGO can increase the volume of the sky covered by 3.2 times as compared with only the power-recycled LIGO detectors - (thus proportionately increasing the event rate) - and by 1.7 times the sky covered by the power-recycled LIGO-VIRGO network. For the detection of burst sources of a given energy, we find that a network of power-recycled LIGOs with dual-recycled GEO and AIGO can increase the volume of the sky covered by 4.9 times as compared with only the power-recycled LIGOs. These values for both the cases are of course far less than the range that can be covered by only the LIGO-VIRGO network with dual recycling operation at a later stage, but the accuracy in the determination of direction, distance and other source parameters will be much better in a coincidence experiment in which other detectors and especially AIGO take part.

04.80.Nn, 95.85.Sz, 97.60.Bw, 97.80.-d

arXiv:gr-qc/9509042v1 22 Sep 1995

I. INTRODUCTION

The direct detection of gravitational waves is perhaps the most challenging problem in experimental physics today. Efforts initiated by Weber [1] with bar detectors and followed up by several individuals and research groups in various directions [2,3] over the last three decades towards achieving this goal are now culminating into the planning and setting up of long baseline laser interferometric gravitational wave detectors in several countries around the globe. The prototypes of these already exist in Germany, Great Britain, Japan and USA.

We can expect that at the turn of the century we shall have a network of three long baseline laser interferometric gravitational wave detectors as a result of the successful accomplishment of the American LIGO (4 Km length) [4] and French-Italian VIRGO(3 Km) [5] projects. Two more detectors, GEO (600m) [6] in Germany and TAMA (300m) in Japan are under construction. Also, a 500m detector, AIGO is in the planning stage in Australia.

The most promising sources to be detected by the planned long baseline interferometers are the compact coalescing binary systems which emit a typical *chirp* like waveform. Because of their inherent broadband nature, interferometric detectors can be used to follow the changing frequency of this wave emitted during the inspiral of compact binary systems during the final stages of their evolution. The rate of such coalescences is estimated to be about three per year out to a distance of 100-200 Mpc [7]. The problem of detection of the gravitational wave signal from a coalescing compact binary and estimation of its parameters for a single detector has been studied by a number of authors [8–13]

For confirming the detection of gravitational waves it is essential to conduct coincidence observation by checking the consistency of the responses of two or more detectors at different sites to a gravitational wave event to eliminate rare and unmodelled sources of noise in single detectors. Also, once the instruments achieve their first objective of detecting the gravitational waves, then the whole network can serve as a powerful astronomical observatory providing

information complementary to that obtained by means of electromagnetic wave observations [14–17]. An important problem called the inverse problem is to determine from the response function obtained by means of linear filtering of the data in each detector the astrophysically important parameters, i.g., the distance to the binary, its orientation and position in the sky, masses and spins. Solutions to this problem have been arrived at for detector networks, both in absence of noise [18] and in presence of noise [19,20].

Since a network of three detectors provides three amplitudes and two independent time delays, it is the minimum configuration needed to determine the five parameters of the gravitational waves, namely, two angles representing direction, two independent polarizations, h_+ and $h_\times$ in the geocentric coordinate system and the orientation of polarization angles on the sky, ψ. Two independent relative time delays, in turn, however, yield two source directions. So, a complete solution for the gravitational wave requires observation by four laser interferometric broadband detectors. This provides another advantage over three detector network: in coincidence experiments with four detectors, the solution for a transversely polarized quadrupolar wave will be overdetermined and thus any inconsistency among the data would be evidence for other polarizartion states [19]. One can, therefore, test Einstein's predictions regarding gravitational wave polarization using such a network.

The responses, $h_+(t)$ and $h_\times(t)$ given by the interferometers to a source can be calculated as a function of the absolute distance and other parameters of the binary system. So, by measuring these responses it is possible to calculate the absolute distance of the source [14–16,19–22], the orientation of the orbital plane (but only with an order four symmetry) [21] and the masses and spins of two bodies [22]. As pointed out by Schutz [15–17] and later studied in detail by Marković [23], the determination of the distance of the binary will also lead to an accurate measurement of the Hubble's constant and other cosmological parameters of our universe.

In this paper, however, we re-address the problem of the detection of broadband gravitational waves from the coincidence observation of the possible networks of the planned interferometric detectors and set the thresholds for the planned detectors for the observation of both burst and *chirp* waveform from compact coalescing binaries. So, we consider simple threshold crossing experiments, in which coincidences are sought between times when the detector outputs cross preset thresholds. This problem was first discussed by Schutz [24], but here we investigate how exactly one should take into account different sensitivities of the planned detectors and time delays between them to formulate an optimal way to set the thresholds.

The study of the coincidence experiment among the planned detectors is very important also due to the following reason: if the source lies anywhere near the plane formed by the LIGO/VIRGO network, the accuracies of their direction measurements and the ability to monitor more than one waveform will suffer a lot [3]. The coincidence experiment with a fourth detector at a site far out of this plane is very important to get a good sky coverage and for the accurate determination of source parameters. The sites chosen for the Australian detector, AIGO and the Japanese detector, TAMA fit nicely into these criteria. We now investigate here, by taking other related factors into consideration, like sensitivities, how this network of the planned detectors would turn out to be useful.

We note here that the thresholds for the detectors in a particular network are to be set at a level which will guarantee with some level of confidence that any collection of events above the thresholds of all the detectors will be free from contamination of 'false alarms'. The calculation to determine threshold levels for any coincident experiment should take into account the following three considerations [24]:

(a) *Difference in sensitivity of the detectors*: If $\mathcal{T}_1$ is the threshold of detector 1 which we consider to be the reference one, then, in order to detect the same gravitational wave, one should set the threshold of detector $\jmath$ at $\zeta^\jmath \mathcal{T}_1$, where $\zeta^\jmath$ is the ratio of the signal to noise ratios of detectors $\jmath$ and 1 for gravitational waves from a particular kind of source. So, the false alarm rate for the coincidence experiment is kept down mainly by lowering the rate of the noise-generated accidental events in the more sensititive detector.

(b) *Time-delay window size*: If two detectors are separated by some distance, then events generated by noise within a certain time-delay window between detectors will contribute to the false alarm rate. If $\mathcal{F}$ is the chosen value of the joint rate of false alarm to which we want to set our detectors and if the maximum time delay between the detectors is $W/2$ measurement intervals, then, for calculation of the threshold, the appropriate probability to use is $\mathcal{F}/W$, since each possible event has to be compared with W possible coincident ones in the other.

(c) *The effect of filtering the data on the setting of thresholds*: Filtering is an important aspect for the detection of signals from coalescing binaries, whereas in case of short duration bursts the detection process has to depend on the time-series observation.

In section II, we give a short description of the planned laser interferometric detectors and present the values of various important parameters used in the design of these interferometers and make comparisons of their sensitivities for coalescing compact binaries and millisecond burst sources. Section III describes our calculation of the optimum window size for networks with detectors at three or more different sites. In section IV we discuss the effect of filtering

on setting thresholds for the observation of coalescing binaries and make a conservative estimate of the number of filters to be chosen for our calculation. Finally, we set the thresholds for detectors in different networks for the observation of two kinds of sources mentioned above and also present values of range as well as the source rate that can be achieved by these networks. In section V we summarize our results and make some concluding remarks.

Unless stated otherwise, we work with units in which $G = c = 1$, so that all quantities are expressed in units of seconds. Sometimes, for convenience, we express masses in unit of solar mass, the conversion factor being $1M_\odot = 4.926 \times 10^{-6}$ sec.

II. DESCRIPTION OF DETECTORS AND THEIR RELATIVE SENSITIVITIES

Table I provides a short description of the site and configuration of the planned detectors. The letter written in the second column represents the corresponding detector throughout our analysis. We, however, use the letter H to denote the two LIGO detectors at Hanford together. It should also be noted that the 300m TAMA (Tokyo Advanced Medium-scale Antenna) has been designed to work as a prototype in its initial stage. The minimum length of the proposed AIGO detector has been set to be 500m, however, this may change, but not much, depending on the budget available [25]. It may be noted that AIGO is the only detector to be built up in the southern hemisphere.

In the analysis that follows we *only* consider the initial LIGO detectors and *not* the advanced ones. One of our main objectives here is to analyse how well the network of the six detectors can be used for the detection of gravitational waves in near future. The global network may completely change by the time the advanced detectors come up and then a similar analysis can again be repeated taking into account higher sensitivities and perhaps changed time-delay windows with newer detectors.

The interferometer, in essence, is a rather elaborate transducer from optical path difference to output power. So, by monitoring the change in output power, it would be possible to detect the changing curvature of spacetime induced by the passage of a gravitational wave. To increase the storage time of laser light in arms, either delay lines (DL) [26] or the Fabry Perot (FP) [27] cavity system has to be adopted, both of which have certain advantages and disadvantages associated with them. However, the advantages of having a smaller vacuum system and the possibility of accomodating more than one detector in the same enclosure have led to the choice of the FP system in the long baseline interferometers.

In order to reduce the shot noise level, an integral feature of these detectors will be the use of a high power laser, in conjunction with variants of optical technique known as light recycling. The first one of these techniques is called *power recycling* [28,29], in which, at a dark fringe operation of the interferometer, the outgoing laser light is recycled back into the interferometer by putting a mirror in front of the source, thus enhancing the laser power. When a gravitational wave passes through an interferometer, it modulates the phase of the laser light, thus producing sidebands which travel towards the photodetector [30]. So, another variant of optical technique called *dual recycling* incorporates a second mirror called the *signal recycling mirror* placed in front of the photodetector. This arrangement can store signal sidebands for sufficiently long times to allow optimum photon noise sensitivity within a restricted bandwidth [31]. If one makes one of the sidebands resonant with the three mirror signal recycling cavity (two end mirrors and the signal recycling mirror), the arrangement is called *the narrowband mode of operation*. If the same recycling cavity is made to be resonant with the laser light, that is called the *broadband mode of operation*. Wider the band, lesser the sensitivity [12,31]. One may adjust this by choosing suitable values of the reflectivity of the signal recycling mirror.

In our analysis we consider two kinds of sources: millisecond bursts and the *chirp* waveform from coalescing compact binaries. The Fourier transform of the Newtonian *chirp* waveform, under the stationary phase approximation, is given as

$$\tilde{h}(f) \simeq \begin{cases} Q\mathcal{D}^{-1}\mathcal{M}^{5/6} f^{-7/6} \exp[i\Psi(f)], & \text{for } f_u \geq f > 0, \\ \tilde{h}^*(-f) & \text{for } -f_u \leq f < 0, \\ 0 & \text{for } |f| > f_u, \end{cases} \tag{2.1}$$

where the phase

$$\Psi(f) = 2\pi f t_c - \phi_c - \frac{\pi}{4} + \frac{3}{4}(8\pi\mathcal{M}f)^{-5/3}. \tag{2.2}$$

and f_u represents the approximate value of the frequency at which the inspiral waveform will *shut off*. This happens at an orbital radius of approximately $6.0M$ where M is the total mass of the binary. So, f_u is given by

$$f_u = (6^{3/2}\pi M)^{-1}. \tag{2.3}$$

The function $Q(\theta, \phi, \psi, \imath)$ is dependent on the direction of the source, (θ, ϕ), the inclination angle of binary, $\imath$ and the polarization angle, ψ. The chirp mass of the binary $(= \mu^{3/5} M^{2/5})$ is denoted by $\mathcal{M}$ and μ is the reduced mass. The quantities, $\mathcal{D}$ and t_c represent the distance of the binary and the *collision time* of the system (at which the orbital radius goes to zero) respectively and ϕ_c is the phase of the waveform as it approaches the collision time, t_c.

The signal to noise ratio(SNR) squared can be calculated to be [11,22]

$$(S/N)^2(f) = 4\frac{Q^2 Q_\jmath^2}{D^2}\mathcal{M}^{5/3}\int_{f_l}^{f_u}\left[f^{7/3}S_h(f)\right]^{-1} df, \tag{2.4}$$

where the additional factor, $Q_\jmath$ is inserted to take into account the dependence of the detected waveform on the orientation of the detector, $\jmath$, since we will be considering a network of detectors which, in general, would have different orientations. We will discuss about our choice of the lower and upper frequency cut-offs, f_l and f_u after the Eq.(2.13) below. We also make an important assumption here that the noise of the detector is described by a Gaussian density distribution. The noise power spectral density, $S_h(f)$ is given by

$$S_h(f) = S_h^{\rm seis}(f) + S_h^{\rm susp}(f) + S_h^{\rm int}(f) + S_h^{\rm shot}(f) + S_h^{\rm quan}(f). \tag{2.5}$$

All the terms of the above expression are discussed below.

The thermal noise has contribution mainly from two sources, the pendulum suspension and internal vibration of the test masses. These are given by Eqs.(4.3) and (4.4) respectively in Finn and Chernoff [11] (for detailed discussion, see Saulson [32] and the analysis by VIRGO project [5]) ignoring both torsional and violin modes which contribute to the interferometer signal directly only if the resonant optical mode is misaligned from the central axis of the mirror (see Gillespie and Raab [33]) :

$$S_h^{\rm susp}(f) = \frac{2k_B T f_0}{\pi^3 m Q_0 L^2\left[(f^2 - f_0^2)^2 + (f f_0/Q_0)^2\right]}, \tag{2.6}$$

$$S_h^{\rm int}(f) = \frac{2k_B T f_{\rm int}}{\pi^3 m Q_{\rm int} L^2\left[(f^2 - f_{\rm int}^2)^2 + (f f_{\rm int}/Q_{\rm int})^2\right]}, \tag{2.7}$$

where T, m, Q_0 and f_0 are the temperature, mass, suspension quality factor and resonant frequency of the test mass. The values of T and f_0 are taken to be same for all the detectors, 300^0K and 1 Hz respectively. The test mass fundamental mode and quality factor are represented by $f_{\rm int}$ and $Q_{\rm int}$ respectively.

It may be noted that only the fundamental vibrational mode has been considered in Eq.(2.7) to evaluate the thermal noise due to the internal vibration. A more accurate estimation should include more number of modes to predict the Brownian motion of the mirror surface (see the detailed analysis by Gillespie and Raab [34]). However, the internal thermal noise will not be a serious contributing factor to the overall noise curve of the first LIGO interferometers; but it is likely to be a serious contributor in advanced interferometers. Typically, more modes can contribute to thermal noise for larger mirrors and smaller laser beam spot sizes [34].

Both the above expressions have been obtained by assuming that the noise would be due to viscous damping rather than structural damping. Works by various groups [5,32–34] suggested, but did not prove that the primary dissipative force may be due to a phase lag between the stress and strain in both the pendulum suspension and the internal vibrations of the test masses. But this will not be an important issue when applied to the initial interferometers and thus such an assumption will not affect our results in this paper.

The idealized expressions for the photon shot noise for FP and DL type interferometers using power recycling are given by Krolak, Lobo and Meers [12,13], Eqs.(3.5) and (3.6) :

$$S_h^{\rm shot}(f)|_{\rm FP} = \frac{\hbar\lambda}{\eta I_0}\frac{A^2}{\ell} f_c\left[1 + \left(\frac{f}{f_c}\right)^2\right], \tag{2.8}$$

$$S_h^{\rm shot}(f)|_{\rm DL} = \frac{\hbar\lambda}{\eta I_0}\frac{A^2}{\ell} f_d\frac{(f/f_d)^2}{\sin^2(f/f_d)}, \tag{2.9}$$

where I_0, λ are laser power and wavelength, η is the quantum efficiency of photodiode, A^2 represents mirror losses, ℓ is the detector arm length. The quantity f_c represents the frequency at which the detector sensitivity has its optimum

shot-noise limited values and is called the *recycling knee frequency*. It can be adjusted by choosing appropriate value for the input mirror reflectivity of the cavity:

$$f_c = \frac{(1-\sqrt{R_1 R_2})c}{4\pi\ell}, \tag{2.10}$$

R_1 and R_2 being the intensity reflectivities of the input mirror and the end mirror respectively. Similarly, in DL antennas, the minimum noise spectral density corresponds to a frequency $\simeq 1.2 f_d$ and f_d can be adjusted by choosing the number of bounces, N for a DL system:

$$f_d = \frac{c}{\pi N \ell} \tag{2.11}$$

For the dual recycling mode of operation, where one can work with a narrower bandwidth, Δf around some properly selected frequency, f_n by adjusting the reflectivity of the signal recycling mirror, the photon counting noise has the following expression for both FP and DL system:

$$S_h^{\rm shot}(f)|_{\rm dual} = \frac{4\hbar\lambda c}{\pi\eta I_0}\left(\frac{A^2}{\ell}\right)^2\left[1+4\left(\frac{f-f_n}{\Delta f}\right)^2\right]. \tag{2.12}$$

It should be noted at this point that the expressions presented above provide only some idealized numbers for the values of the shot noise. In reality the situation would be somewhat worse due to the phase modulation technique [35] to be incorporated in these interferometers. The phase modulation technique is necessary in practice to overcome the effects of imperfect fringe visibility and to move the signal away from low frequencies where the laser light tends to have excess noise.

Also, the contribution of the quantum uncertainty in the determination of the periodic motion of the end masses is given by (see Eq.(121), Ref. [2])

$$S_h^{\rm quan}(f) = \frac{8\hbar}{4\pi^2 f^2 \ell^2 m}. \tag{2.13}$$

So far we have not considered the seismic noise. The amplitude of the seismic noise depends on local characteristics of the seismic displacement noise at the site as well as the nature of the seismic isolation circuit and, obviously, will be different for different detectors (see Saulson [36] and Eq.(4.6) of Ref. [11]). The seismic noise spectrum falls very steeply ($\sim f^{-24}$) and is like a 'wall' near a certain frequency which we call f_l. So, practically for $f > f_l$, the seismic noise contribution is negligibly small as compared to the thermal noise and the shot noise, while for $f < f_l$, $S_h^{\rm quan}(f) \to \infty$. We uniformly choose f_l to be 70 Hz for all the detectors for the purpose of data analysis, however, in reality, this may vary. If the seismic noise characteristics for all the detectors get properly determined, then, of course, one can incorporate this noise in the expression for $S_h(f)$ and may choose a much lower value for f_l to calculate the relative SNRs to be defined in Eq.2.14 below.

We checked numerically that, if the seismic noise is considered to be negligible above the chosen value of f_l, then according to the calculation done by us, variation in the choice of f_l within the range (10Hz - 100Hz) does not change the value of the relative SNR much (as defined in the following Eqs.2.14 and 2.16) for all the detectors in their initial stage. We also choose $f_u = 2000$ Hz in our calculation of relative SNRs which correspond to a total mass,$M = 2.2 M_\odot$ of the binary system.

We may note that although we have neglected the seismic noise above a certain frequency, f_l, we have not neglected the quantum noise, $S_h^{\rm quan}(f)$ which is also quite small there. The reason is that above frequencies much greater than the pendulum frequency, f_0 (=1Hz), the seismic noise falls as steeply as f^{-24}, whereas the quantum noise falls as f^{-2}. So, the latter may become important in a narrower-band dual recycling operation with a low value of f_n and may act as the fundamental limit to the sensitivity of the narrow band operation. For a power recycling operation, of course, both may be neglected above f_l.

Now, referring to the expression for SNR given in Eq.2.4, we can define the relative signal to noise ratio of any detector ȷ (≡ L, H4, H2, V, G, T or A) for a particular binary system by normalising its own value with that of any of the LIGO full-length detectors:

$$\zeta_{\rm cb}^{\rm J} = \left[\frac{F_{\rm cb}^{\rm J}}{F_{\rm cb}^{L}}\right]^{1/2} \tag{2.14}$$

where the subscript 'cb' represents coalescing binary and

$$F^{\mathrm{J}}_{\mathrm{cb}} = \int_{f_l}^{f_u} \left[f^{7/3} S^{\mathrm{J}}_h(f) \right]^{-1} df \tag{2.15}$$

and $S^{\mathrm{J}}_h(f)$ represents the noise power spectral density of the detector J. In this first analysis we have ignored the orientation factors of the detectors, that is in effect we have taken Q_{J} to be same for all the detectors. Statistically, an averaging effect would be present if we assume isotropic distribution of sources.

To arrive at some close-to-real values of the relative SNRs for the burst sources, in the absence of our knowledge of the waveform, we assume the power of the burst to be distributed uniformly in a frequency range between 70 Hz and 2000 Hz; The level of this power spectrum is different for different sources. Then, for any particular burst source, the relative SNRs as normalized to that of a full-length LIGO can be given as

$$\zeta^{\mathrm{J}}_{\mathrm{bur}} = \left[\frac{F^{\mathrm{J}}_{\mathrm{bur}}}{F^{L}_{\mathrm{bur}}} \right]^{1/2}, \tag{2.16}$$

where

$$F^{\mathrm{J}}_{\mathrm{bur}} = \int_{f_l}^{f_u} \left[S^{\mathrm{J}}_h(f) \right]^{-1} df \tag{2.17}$$

In Table II we present values of the different parameters we used in our numerical calculation to arrive at the values of the relative SNRs, $\zeta^{\mathrm{J}}_{\mathrm{cb}}$ and $\zeta^{\mathrm{J}}_{\mathrm{bur}}$. In most of the cases, especially for VIRGO [37], GEO [38], AIGO [25] and TAMA [39], these have been obtained by personal communication with people involved in designing the planned detectors. The values for LIGO have been taken from Ref. [4]. Some of these are quoted as *conservative estimates*, while others are quoted to be *hopefully achievable ones*. A few of the values are assumed by us. The value of R_1 for H2 has been chosen such that its cavity finesse becomes approximately twice that of H4 [40]. This leads to the same value of recycling knee frequency for both the detectors.

Table III presents the values of $\zeta^{\mathrm{J}}_{\mathrm{cb}}$ and $\zeta^{\mathrm{J}}_{\mathrm{bur}}$ obtained by us for both power and dual recycling mode of operation. *We should note that all values, including those obtained for the dual recycling operation are normalised with respect to the SNR of power recycled full-length LIGO for the same kind of source.* The dual recycling parameters are, in all cases, chosen to be those for a bandwidth of 300Hz around 250Hz as will be used in GEO [38]. It should be noted that for different detectors, maximum gain may be obtained for different values for bandwidth and central frequency [41]. Although the dual recycling values for LIGO, VIRGO and TAMA have been calculated, they do not have any plan for implementing this in their initial interferometers.

The values of the SNR of VIRGO for the burst waveform in TableIII may seem to be too high as compared to those for other detectors. As we guess, the reason for such a high value may be the choice of a high value for the recycling knee frequency, f_c, (~ 620 Hz) as compared to that of LIGO (~ 92 Hz), which leads to a lower value for VIRGO of the noise at high frequencies (where it is shot-noise-limited). Since the power of the burst waveform is assumed by us to be uniformly distributed in a frequency range 70-2000 Hz, the SNR as calculated for VIRGO turns out to be more.

We have also checked that, as mentioned above, if the seismic noise is considered to be negligible, the value of $F^{\mathrm{J}}_{\mathrm{cb}}$ (SNR is proportional to the square root of this) does not change much as one goes to lower values of f_l. For full-length LIGO with power recycling, this value increases by only 3.6% as the value of f_l is reduced from 70Hz to 10Hz and reduces by 6% as f_l is increased from 70Hz to 100Hz (the value of F^{L}_{cb} for $f_l = 70$Hz is 5.01×10^{42}). The variations in the relative SNRs of other detectors are even less. The reason for this is the high value of thermal noise at the low frequency range for all the detectors at their initial stage, which prevents the SNR to grow much. However, the seismic noise and the choice of f_l will be very important once the thermal noise is reduced to a sufficient extent.

III. DETERMINATION OF THE WINDOW SIZE

In this analysis, we confine our attention typically to bursts of duration 1 msec. Then we must sample the noise in the output effectively 1000 times per second and should set the thresholds of the detectors such that the *false alarm rate*, $\mathcal{F}$ for the coincident observation does not go beyond *1 measurement per year*.

We differ from Ref. [24], while calculating the time delay window size for three or more detectors. If $W/2$ is the maximum of the values of time delay between the detectors, then following that analysis, one can overestimate the window area as the area of the square, W^2. We optimize this case and obtain a much reduced window area by calculating the possible range of the window length between 3rd and 1st detector by fixing each time the window length between 2nd and 1st. The procedure we follow is explained in detail below. The method of optimization followed by us gives its best results for networks of four or more number of detectors.

Since in this analysis we are mainly interested in the problem of detection by coincidence experiments and not in the more involved problem of determination of the exact direction and other parameters, we choose to work with a coordinate system which is fixed with respect to a particular detector network. The detectors have different orientations on the surface of the earth and also the waves will arrive from random directions with random polarization angles. The antenna pattern and the coincidence probability for a detector network averaged over all possible thresholds was computed by Tinto [42] using Monte Carlo methods and integrating over all the random parameters. In this paper, however, we are mainly concerned about setting thresholds for the detection of individual events and, therefore, to avoid complications, we completely ignore the fact that different detectors would respond differently to a given gravitational wave.

A. window size for three detectors

As shown in Fig.1, let us take the line joining detectors D_1 and D_2 to be the z axis. Let n_2 be the time delay, in units of sampling interval Δ, in the arrival times of the gravitational wave between D_1 and D_2 :

$$n_2 = (t_2 - t_1)/\Delta, \qquad -N_2 \leq n_2 \leq +N_2, \tag{3.1}$$

where t_1 and t_2 are arrival times at detectors D_1 and D_2 respectively; Δ represents the sampling interval. The quantity N_2 $[= d_{12}/(c\Delta)]$ represents the maximum time delay in terms of measurements ($c \rightarrow$ the velocity of light, $d_{12} \rightarrow$ distance between D_1 and D_2). The calculated values for the maximum time-delay (N_2) between two of these detectors are given in Table IV.

Corresponding to each value of n_2, one can determine the polar angle, θ of the direction of wave:

$$\theta = \cos^{-1}(n_2/N_2). \tag{3.2}$$

One can now draw an imaginary circular disk, orthogonal to the z axis, with center at any point C_2 on the axis, so that the line joining D_1 and any point on the circumference of the circle makes an angle, θ with the z axis, as shown in Fig.1.

Now we extend the line joining detectors D_1 and D_3, so that it crosses the disk at point C_3. Let us take our x axis to be the line joining C_2 and C_3. If some point S on the rim of the disk represents the actual direction of the gravitational wave, then the azimuthal angle, ϕ, of this direction will be that between x axis and the line joining points C_2 and S.

If β_3 is the angle between lines, $\overline{D_1C_3}$ and $\overline{D_1S}$, then the time-delay of the gravitational wave in arriving D_1 with respect to D_3 can be given by $n_3 = N_3 \cos\beta_3$, where N_3 is the maximum time-delay between D_1 and D_3. The angle β_3 can be expressed in terms of angles θ, ϕ and α_{23} which is the angle between lines $\overline{D_1C_2}$ and $\overline{D_1C_3}$. We thus obtain

$$n_3 = N_3 \cos\theta(\cos\alpha_{23} + \sin\alpha_{23}\cos\phi\tan\theta). \tag{3.3}$$

The maximum and minimum value of n_3 can be obtained when $\phi = 0$ and π respectively. In those cases, after some manipulation, we arrive at

$$n_3^2 + n_2^2(p^2 + q^2) - 2pn_2n_3 - q^2N_2^2 = 0, \tag{3.4}$$

where $p = (N_3/N_2)\cos\alpha_{23}$ and $q = (N_3/N_2)\sin\alpha_{23}$. This is the equation of an ellipse that thus represents the circumference of the surface of the required time delay window for three detectors, as shown in Fig.2 for the (H, L, V) network. As shown in Fig.3, for any particular value of n_2 (say, 15), the value of n_3 may vary in between $N_3\cos(\theta + \alpha_{23})$ and $N_3\cos(\theta - \alpha_{23})$, depending on ϕ.

The window space is actually a lattice since the possible time delays are integer multiples of the finite sampling time that we consider. The area of this elliptical window is calculated to be

$$\text{Window size(3 sites)} = \pi N_2 N_3 \sin\alpha_{23} = 2\pi \times \text{Area of triangle joining three detectors}, \tag{3.5}$$

which is an invariant quantity for any three detectors, irrespective of the labelling of the detectors. The choice in labelling is, however, important for the reason we discuss below.

We present values of the optimum window sizes for different networks of any three planned detectors in Table V. It may be noted at this point that for the approximate calculation presented in Ref. [24], the window size for three detectors was overestimated to be the square of the largest value among the three maximum time-delays expressed in number of measurements. Our results show that the optimum window areas calculated in this way can be, for

example, as low as below 10% of their respective maximum window areas for (H,V,G), (L,V,G), (V,G,A) and (V,G,T) networks.

We note that if a particular combination of n_2 and n_3 is known, one can determine the azimuthal angle for the direction of gravitational wave, ϕ to be any of these two possible values:

$$\phi = \pm \cos^{-1}\left[\frac{N_2 n_3 - N_3 n_2 \cos\alpha_{23}}{N_3\sqrt{N_2^2 - n_2^2}\sin\alpha_{23}}\right]. \tag{3.6}$$

Along with Eq.3.2, this provides two possible direction of the source.

B. window size for four or more detectors

As mentioned in section I, the four detector problem is over determined. The calculation of window size depends on the procedure we follow. If we measure the event amplitudes for four detectors then, in principle, we need only one time delay to determine the solution that involves five parameters and then we can reject noise-generated events whose other time delays are not consistent with this solution. We, however, would first like to check the consistency among the four time delays and then measure the individual event amplitudes. This also provides us an opportunity of testing Einstein's predictions regarding the polarization states [19].

Let us now extend the line joining D_1 and detector D_4, so that it crosses the imaginary circular disk at point C_4. Then the time delay of the gravitational wave in arriving D_1 with respect to D_4, is $n_4 = N_4\cos\beta_4$, where N_4 is the maximum time delay between D_1 and D_4 and β_4 is the angle between lines, $\overline{D_1C_4}$ and $\overline{D_1S}$. Expressing β_4 in terms of other angles, we can write

$$n_4 = N_4[\cos\alpha_{24}\cos\theta + \sin\alpha_{24}\sin\theta\cos(\psi - \phi)], \tag{3.7}$$

where ψ, the angle between the x axis and the line joining points C_2 and C_4, can be expressed as

$$\psi = \cos^{-1}\left[\frac{\cos\alpha_{34} - \cos\alpha_{24}\cos\ alpha_{23}}{\sin\alpha_{23}\sin\alpha_{24}}\right]. \tag{3.8}$$

Any angle α_{ij} $(i, j = 2, 3, 4)$ in above expresssions represents the angle the line joining detectors D_i and D_1 make with that joining D_j and D_1.

So, corresponding to every set of values for (n_2, n_3), there can be two possible values for n_4 depending on ϕ :

$$n_4 = Xn_2 + Yn_3 \pm Z\sqrt{K + Pn_2n_3 - Qn_2^2 - n_3^2}, \tag{3.9}$$

which has been obtained using expressions for θ and ϕ in terms of n_2 and n_3 and where the constants for a specific set of detectors are represented by

$$\begin{aligned}
X &= \frac{N_4}{N_2}(\cos\alpha_{24} - \sin\alpha_{24}\cot\alpha_{23}\cos\psi),\\
Y &= \frac{N_4}{N_3}\csc\alpha_{23}\sin\alpha_{24}\cos\psi,\\
Z &= \frac{N_4}{N_3}\csc\alpha_{23}\sin\alpha_{24}\sin\psi,\\
K &= N_3^2\sin^2\alpha_{23},\\
P &= \frac{2N_3}{N_2}\cos\alpha_{23},\\
Q &= \frac{N_3^2}{N_2^2}.
\end{aligned} \tag{3.10}$$

One can now do some algebraic manipulation starting with squaring both sides of Eq.(3.9) to finally arrive at the equation of the surface of an ellipsoid which is rotated with respect to its coordinate axes. The two equations in Eq.(3.9) with (+) and (−) sign in front of the square root represent two halves of the ellipsoidal surface. Fig.4 shows this surface for the AHVL network with A as the reference detector.

The events that may lead to the false alarm will be points distributed on such a surface. So, once we choose the reference 3-detector subnetwork, the window size for the 4-detector network would be the number of lattice cells on the ellipsoid which is twice the window size for the first three detectors.:

$$\text{Window size(4 sites)} = 2\pi N_2 N_3 \sin\alpha_{23} = 4\pi \times \text{Area of triangle joining 3 reference detectors,} \tag{3.11}$$

We observe that the maximum window size of a three dimensional volume ($= W^3$), where $W/2$ is the maximum of the values of time delay among the detectors gets reduced to the area of a two dimensional surface in three dimensions. We can, therefore, expect that the optimization would help to a substantial extent in reducing the threshold level calculated otherwise using maximum window area.

Now we address the question how one should select the reference subnetwork of three detectors out of four possible choices. We can have two criteria of selection: (i) The window area of the reference subnetwork should be as low as possible to avoid increase in the false alarm rate; (ii) the unavoidable presence of uncertainty in measurements of the time delays will always allow some room in the window for noise-generated events. So, the reference subnetwork should be chosen in such a way that the error in determining the direction of the source from its time-delay data is as low as possible.

From Eqs.(3.2) and (3.6), we note that the accuracy of the determination of direction improves with larger values of N_2, N_3 and α_{23} for given values of error, Δn_2 and Δn_3. So, it is always better to choose the reference detector in such a way that these values take the largest possible ones. One has to make a good choice by considering all three possible sets of values. These selection criteria for achieving smaller errors in the determination of the direction of source, however, go against a choice based on the smallest window size: The accuracy is the best for the 3-detector subnetwork with the largest window area.

Since these two criteria make diametrically opposite demands on the window size, we would consider their quantitative effects. Referring to Table V, for example, one can see that for the AHVL network, the highest possible window size corresponding to the reference subnetwork, AHV is about 3.7 times the lowest possible window size corresponding to the reference subnetwork, VHL. Since the threshold would be normally at quite high level (say, 7σ or even higher; see next section for more discussion and the definition of σ, the standard deviation of noise), increasing the window size by a factor of 3 or 4 has only a small effect on the thresholds, but it could lead to dramatic improvement in the accuracy for determining the direction of the source.

We, therefore, ignore the criterion (i) and follow only the criterion (ii) for making our selection for the reference detector and the reference subnetwork of three detectors. So, for example, in case AIGO is a member of the four detector network, we would always like to choose it as the reference one (the D_1) simply because it is always at the farthest distance from any of the detectors. Similarly, we would also choose H to be another member of the reference subnetwork because this provides another half-length detector at the same site and thus extra advantage in coincidence detection. So, as an example, for (AHVL) network, our choice of the reference subnetwork is (AHV). We choose V instead of L because the angle α_{23} is the largest in this case. From now onwards, whenever we refer to a network of four or more detectors, the first three names written will represent our choice of the reference subnetwork and the first name will correspond to the reference detector.

Once one does observation with a four detector network one determines the direction of the source and thus if a fifth detector is available, one just has to check whether or not the time of arrival in that is consistent with the values of the four-detector network. So, we can conclude that the optimum window size for a network with detectors at five or more different sites is again just twice the size of the window for the reference 3-detector network.

IV. SETTING THRESHOLDS FOR DETECTORS

We assume that in the output x of any of the detectors, J, the only noise source is stationary and characterised by the Gaussian Normal distribution, with zero mean and standard deviation, σ_{J}. The values of σ_{J} are, of course, different for different detectors. So, the probability that the output x will exceed some fixed threshold value, X_0 is given by

$$\begin{aligned} P(\mid x \mid > X_0) &= 1 - 2\int_0^{X_0} \frac{1}{\sqrt{2\pi}\sigma_{\mathrm{J}}} \exp[-x^2/(2\sigma_{\mathrm{J}}^2)]\, dx \\ &= \mathrm{erfc}(\mathcal{T}_{\mathrm{J}}/\sqrt{2}), \end{aligned} \tag{4.1}$$

where

$$\mathcal{T}_{\jmath} = \frac{X_0}{\sigma_{\jmath}} \tag{4.2}$$

which, from, now onwards will be referred to as the value of the *threshold* set in the detector ȷ. The $\sigma_{\jmath}$ here is the value of the standard deviation of the noise averaged over the bandwidth of the detector. For the white noise case, for example, $(\sigma_{\jmath})^2$ is just the bandwidth divided by $F^{\jmath}_{\rm bur}$.

It is advantageous to choose a low threshold, and correspondingly high false alarm rate for the less sensitive detectors. The noise-generated accidental coincidence rate is kept down mainly by the lower rate of false alarms in the more sensitive detectors. So, we keep the value of the output X_0 corresponding to the threshold to be same in all the detectors. As pointed out in section III, this assumption ignores the fact that different detectors will actually give different responses to a gravitational wave depending on their orientations on the surface of the earth and the direction and polarization angle of the wave.

So, if X_0 is kept at the same level in different detectors by neglecting the above-mentioned effect, the values of $\mathcal{T}_{\jmath}$ is to be set at different values in different detectors. If $\mathcal{T}_1$ is the threshold of the first detector, then, in order to detect the same gravitational wave, one should set the threshold of detector ȷ at $\zeta^{\jmath}\mathcal{T}_1$, where $\zeta^{\jmath}$ is the ratio of the SNRs of the ȷ-th and the first detector.

So, on the basis of our discussion in the last three sections, we can now fix the thresholds, $\mathcal{T}_{\jmath}$ in a network having n number of detectors by the following equation:

$$\mathrm{erfc}(\mathcal{T}_1/\sqrt{2}) \prod_{\jmath=2}^{n} \mathrm{erfc}(\zeta^{\jmath}\mathcal{T}_1/\sqrt{2}) = \frac{\mathcal{F}}{W\chi} \tag{4.3}$$

where W is the window size and χ is a factor equal to unity for a burst source and equal to the number of filters, N_f for a coalescing binary signal. We consider a false alarm rate, $\mathcal{F}$, of one per year or 3.171×10^{-11} in our calculation. As our discussion in the following subsections will show, for a single detector observing coalescing binaries, this translates into a threshold value of 7.65, whereas for the same observing millisecond burst sources, the threshold has to be set at 6.64 due to the absence of filtering in the latter case. Also for the purpose of setting setting the threshold, we ignore the correlation between the samples of the statistics used for detection. Although there is some correlation among the samples, the effect on the threshold has been, however, shown to be negligible [43].

We, therefore, decide, that a detector whose sensitivity is less than about one-third of any other detector in the same network does not come to be very useful for the network as such. In that case the false alarm rate of the less sensitive detector would be very high, or equivalently, the noise generated events in that detector would cross the threshold quite often and such a coincidence experiment would not carry any meaning at all. For instance, in case of two detectors, such an experiment would be almost nothing different from the more sensitive detector observing alone.

One can, therefore, guess from these values of $\zeta^{\jmath}_{\rm cb}$ in Table III that the medium scale interferometers (G, A, T) under power recycling operation will not be very useful for a coincidence experiment with the LIGO-VIRGO network. However, as discussed in section II, if they are narrow-banded by dual recycling, say, with a bandwidth of 300Hz around 250 Hz as planned for GEO [38], their sensitivities become comparable, and in some cases, better than that of LIGO or VIRGO with power recycling operation. A meaningful coincidence experiment can, therefore, be performed only under this condition. For the same reason, TAMA, even with its length of 300m, may come to be very useful for the networks of the rest of the planned detectors, especially for obtaining a good sky coverage and accuracy in the determination of the source parameters, once an improved pendulum is incorporated in the design.

A. Thresholds for detecting signals from burst sources

We should recall here that in the absence of our knowledge about the possible waveform of the burst sources, we assumed that the power of burst is uniformly distributed over a frequency range (70-2000)Hz. Setting thresholds for detecting such burst sources is relatively easier as compared to the case of coalescing binary signals due to the absence of filtering. The millisecond burst sources will be detected in coincidence experiments just by checking consistency in the arrival of burst in the time series of different detectors. In this case, we set $\chi = 1$ in the right hand side of Eq.(4.3). So, if we consider a single detector observing millisecond burst sources, for a false alarm rate, $\mathcal{F}$ of one per year, the threshold, $\mathcal{T}$ has to be set at 6.64.

For the model of burst waveform considered by us, we find that the relative sensitivity of the power-recycled VIRGO is quite high as compared to others with their present design parameters and thus, as discussed above, a coincidence experiment performed by including VIRGO in the network would not be a meaningful one.

In Table VI we present the threshold values we have set for different detectors participating in the coincidence experiments of some interesting networks for the observation of millisecond burst sources.

We find that a network of power-recycled LIGOs and dual-recycled GEO and AIGO can increase the volume of the sky covered by about 4.9 times as compared with only power-recycled LIGO detectors for the observation of the burst sources of a given strength. The absolute range of observation will, of course, vary with the strength of the burst.

B. Thresholds for detecting signals from coalescing compact binaries

The choice of the threshold levels for the detection of signals from coalescing compact binaries will differ from that for burst sources due to the effect of filtering. Filtering can have the following three effects on the setting of thresholds:

(i) If it is assumed that there is no correlation in the filter outputs, then N_f number of filters lead to an increased false alarm rate of $(N_f\mathcal{F}_0)$, where $\mathcal{F}_0$ is the false alarm rate when no filter is used. Here we set $\chi = N_f$ in Eq.4.3.

The problem of determination of the lattice of filters for the observation of coalescing binary signals was investigated by Sathyaprakash and Dhurandhar [9] for the white noise case and again by Dhurandhar and Sathyaprakash [10] for the coloured noise case. But, as discussed below, in the present case the problem is somewhat nontrivial, although not very important for setting threshold levels of various detectors.

In order to apply the technique of matched filtering for the detection of the chirp waveform, it is necessary to construct a lattice of filters corresponding to different values of the three parameters in their relevant range. The spacing between filters depends on the allowed value of drop in the correlation function of two *chirp* waveforms with different values of their parameters. It was shown [9] that for the Newtonian chirp waveform, it is sufficient to choose such a set of filters covering only the range of the phase ϕ_c and the chirp mass, $\mathcal{M}$. However, since the correlation of a given data set with a filter of arbitrary phase can always be expressed as a linear combination of the correlation of the same with two independent basis filters corresponding to, say, $\phi_c = 0$ and $\phi_c = \pi/2$, it was shown [9] to be sufficient to construct a lattice with two filters for each value of the mass parameter. Once the correlations are calculated with the basis sets, the phase of the filter which maximises the correlation can be easily calculated by an analytical expression.

However, the spacing between mass parameters for the choice of filters crucially depends on the noise characteristics of the detector. For example, it was found [10] that the consideration of coloured noise in the case of power recycling led to the reduction of the number of filters by approximately half as compared to that considering white noise. This reduction in number is mainly due to the effective reduction of the bandwidth which happens because, in case of recycling, the sensitivity of a detector is enhanced at the lower end of the detector bandwidth at the cost of a greater noise at higher frequencies. This leads to a slow fall-off in correlation and thus to larger spacing between filters.

Since the noise characteristics of different detectors would be different depending on their choice of the knee frequency, laser power, laser wavelength, mirror loss etc., so, strictly speaking, the distribution as well as the number of filters in the lattice can be chosen to be different for different detectors. So, in the present context, we have to define properly what we would call a 'coincidence detection' by analysing the outputs of various detectors in a network.

For a coincidence detection, it is necessary that the filters with the same set of values of the parameters of the chirp waveform in different detectors cross their thresholds at appropriate times. Since the phase, ϕ_c observed by a detector is dependent on its orientation, we neglect the matching in ϕ_c as a criterion for the coincidence detection. So, we consider an event to be a case of 'coincidence detection' if filters with the same value of the mass parameter in different detectors cross their thresholds at appropriate points in time. The information obtained about ϕ_c can be important, however, for a more rigorous second analysis of the data once a decision is arrived on coincidence detection based on the above criterion.

On the other hand, if the same range of the mass parameter is covered by different sets of filters, S_F^{J}, characterised by differently selected values for the mass parameter, then it may so happen that only one detector detects a signal while others miss it due to the absence of the filter corresponding to that particular one in their lattice. But if such a situation arises, the other detectors can then do a reanalysis, searching for the corresponding signal this time. This shows that the set of filters that will actually contribute to the false alarm rate is the union of these different sets for different detectors, i.e., $\bigcup_{\mathrm{J}} S_F^{\mathrm{J}}$.

A detailed analysis leading to the accurate determination of the number of filters for different detectors is, however, unimportant for the main objective of this paper. Our interest in the number of filters is due to its

effect on setting thresholds as mentioned above. We can see that although the order of magnitude of the number obtained by multiplying the window size with N_f is very important for setting the thresholds, a factor of 2 or 3 in the ratio of the number of filters for different detectors does not make much difference in the threshold levels. We, therefore, assume that, to avoid complications, the same number of filters, N_f will be chosen for different detectors participating in the coincident experiment, irrespective of their noise characteristics, thus demanding same computational facility in all the detectors. For example, the number of filters calculated for the most sensitive detector, but with the highest value of the sampling rate (corresponding to the widest bandwidth one likes to consider) may be a good choice for this common number.

For the present analysis, however, we take a conservative estimate of N_f (a maximum value) which can be obtained *by considering the white noise case*. The number of filters obviously depends on the range of chirp mass one intends to cover and for a high value of the upper limit (say, $\mathcal{M} = 20M_\odot$), N_f for the white noise case can be given by Eq.(4.2) of Ref. [9]:

$$N_f = 3000 \left[\frac{\mathcal{M}_1}{M_\odot}\right]^{-5/3} \left[\frac{f_l}{100\text{Hz}}\right]^{-8/3} \left[\frac{\Delta\xi}{1\text{msec}}\right]^{-1}, \tag{4.4}$$

where $\mathcal{M}_1$ is the lower limit on the chirp mass and $\Delta\xi$ is the spacing between the filters corresponding to the values of the chirp mass determined by the following relation between $\mathcal{M}$ and ξ which is referred to as the *sweep time* of the chirp waveform:

$$\xi = 3.00 \left[\frac{\mathcal{M}}{M_\odot}\right]^{-5/3} \left[\frac{f_l}{100\text{Hz}}\right]^{-8/3} \text{sec.} \tag{4.5}$$

The spacing, $\Delta\xi$ is almost a constant for a particular chosen value of the allowable drop in the correlation function between two neighbouring filters. We note that our upper limit of frequency, f_u corresponds to a total mass of the binary, $M = 2.2M_\odot$ and thus a lower limit on the chirp mass, $\mathcal{M}_1 = 1.0M_\odot$ is a suitable choice to make. For an allowable drop in correlation to 0.90 between neighbouring filters, the number of filters is calculated to be approximately 1600. This is the value that we use in our calculation of the thresholds.

It should be noted that the Eq.(4.4) has been evoked here just to get an estimate of the number of filters that may be necessary to detect the coalescing binary signals. However, it should not be taken literally for the actual detectors, since their noise profile differs significantly from the noise modelled to arrive at this equation: white noise for $f \geq f_l$ and a steep wall below f_l.

(ii) On the other hand, if data are filtered, that also reduces the effective noise bandwidth, so the rate at which it needs to be sampled to give an accurate picture of it is less. Since the false-alarm probability depends on how many randomly chosen samples one has, therefore, the rate at which false alarms occur will be less [24].

(iii) The auto-correlation function of the filtered output resembles the sinc function and so, contrary to the assumption made in item(i) above, the adjacent sample points are correlated and, therefore, the filtered output is actually coloured.

These two problems, (ii) and (iii), described above have been studied in detail by Dhurandhar and Schutz [43] and the conclusion is that the reduction of the false alarm rate due to filtering is not much. We can safely ignore these effects in our calculation of the threshold levels.

(iv) The error induced by filtering in exact determination of the time of arrival or time of coalescence of the binary: Any error in determination of these times will lead to a probabilistic region around every lattice point of the window surface and may thus seriously affect our calculation of the window size described in sec. III.

The detailed calculation [44] shows that whereas this error is of the order of ±20-25msec (with 68% confidence) for the time of arrival, the same figure is of the order of ±0.4-0.6 for the time of coalescence for Newtonian and post Newtonian cases. Therefore, it seems to be better to choose the time of coalescence rather than the time of arrival in our window size calculation. In that case the existence of the probabilistic region around the exactly determined window will not contribute much correction to this.

In Table VII we present the threshold values we have set for different detectors participating in the coincidence experiments of some interesting networks for the observation of signals from the coalescing compact binary sources.

We can also calculate the range of observation by these networks by using Eq.(5.8) of Finn and Chernoff [11] which we translate to our case as

$$\mathcal{R}_{90\%} = \left(\frac{\mathcal{M}}{1.2M_\odot}\right)^{5/6}\left(\frac{7.65}{\mathcal{T}_L}\right)\left(\frac{F^{\rm J}_{\rm cb}}{5.0\times10^{42}}\right)^{1/2}\times 37.67{\rm Mpc}. \tag{4.6}$$

One should note that not all sources within a particular range, $\mathcal{R}$ are detectable and, on the other hand, some sources outside $\mathcal{R}$ may come to be detectable. So, $\mathcal{R}_{90\%}$ is defined as the distance within which 90% of the observable sources would lie. The chirp mass, $\mathcal{M} = 1.2M_\odot$ corresponds to, among other combinations, a 1.4-1.4 $M_\odot$ system like the Hulse-Taylor binary pulsar, PSR1913+16.

This leads to a detection rate of compact coalescing binary sources (see Eq.(5.5) of Finn and Chernoff [11]) to be

$$\left(\frac{\dot{\mathcal{N}}}{8\times10^{-8}{\rm Mpc}^{-3}\,{\rm yr}^{-1}}\right)\left(\frac{\mathcal{M}}{1.2M_\odot}\right)^{5/2}\left(\frac{7.65}{\mathcal{T}_L}\right)^{3}\left(\frac{F^{\rm J}_{\rm cb}}{5.0\times10^{42}}\right)^{3/2}\times 4.26\times10^{-3}\ {\rm yr}^{-1} \tag{4.7}$$

The expectation value for the number density of sources per unit time, $\dot{\mathcal{N}}$ was estimated by Phinney [7], which ranges from an ultraconservative value of $\{6\times10^{-10}\}$ Mpc^{-3} yr^{-1} to a conservative estimate of $\{8\times10^{-8}\}$ Mpc^{-3} yr^{-1} and to an upper limit of $\{6\times10^{-5}\}$ Mpc^{-3} yr^{-1}.

We present the values of the range and the rate of detection of coalescing binaries for some interesting networks in Table VIII. We note that a coincidence experiment of power-recycled LIGOs and VIRGO with dual-recycled GEO and AIGO can increase the volume of sky covered by only LIGO detectors by 3.2 times and the same covered by the LIGO-VIRGO network by about 1.7 times. This is of course far less than the range that can be covered by LIGOs and VIRGO with dual recycling operation at a later stage, but the latter case is not very useful for the determination of the direction, distance and other source parameters, as described in sections I and II.

V. CONCLUDING REMARKS

In this paper we investigated how effectively the planned initial interferometeric gravitational wave detectors would be able to detect compact coalescing binaries and burst events and what volume of the sky can be covered by them in the beginning of the next century. Here we summarize our main results:

(i) We made a comparison of the relative sensitivities of all the planned detectors for the observation of both of the above-mentioned sources by taking into account all possible kinds of noise sources which would affect their performance. The numbers obtained by us for the relative SNRs may, however, vary because every detector leaves room for incorporating better techniques to reduce the thermal and the seismic noise. But to a very good approximation these numbers may be taken to be the representative ones for the sensitivities of the detectors in their initial stages. We also calculated relative SNRs for LIGO, VIRGO and TAMA with dual recycling configuration, although they do not have any plan of implementing this in the first stage of their initial detectors.

(ii) From the values of the relative SNRs of different detectors, we find that a meaningful coincidence experiment can be performed if the detectors have similar sensitivities. Thus, if LIGOs and VIRGO are operated in the power recycling mode and all other medium-scale detectors are operated in dual recycling mode, the sensitivities for the detection of the coalescing binary signals become comparable and a meaningful coincidence experiment can be carried out. Similarly, we find that the sensitivity of even the power-recycled VIRGO for the detection of the type of burst sources considered by us (i.e. uniform power spectral density upto 2000 Hz) is quite high as compared to other detectors in their initial stage. So, although VIRGO alone will be able to cover a large volume of sky for the detection of this type of burst sources, it will not come to be useful for a coincidence experiment together with other detectors in a network.

(iii) Next we calculated the time-delay window sizes for networks with all possible combination of detectors. We also set a criterion whereby one should select a reference detector as well as a reference combination of three detectors for the determination of the direction of the source. This is necessary for effectively reducing the error in the determination of the direction of the source: The three reference detectors chosen should form a triangle with maximum area. For example, AIGO should always be chosen as the reference detector since it is always at the farthest distance from any other detector. Similarly, LIGO at Hanford should also be chosen as another member of the reference 3-detector subnetwork because it provides one more detector of 2000m length at the same site and thus extra advantage in coincident experiment.

(iv) We discussed in detail the relevant issues of filtering to calculate the threshold levels for the detection of the coalescing compact binaries. The important issue of how comparison should be made among the outputs of various detectors using different lattices of filters covering the same range of source parameters was also discussed. We finally made a conservative estimate (a maximum number) of the number of filters which would affect the rate of false alarm for the coincidence experiment.

(v) *Threshold criteria for burst sources and coalescing binaries:* We have defined relative sensitivities, ζ^{J} which depend on the type of source and the detector J and in terms of these quantities have set up the threshold levels for two types of sources, namely, (a) burst sources, and (b) coalescing binaries.

(a) In the absence of our knowledge of the possible waveform of the burst sources, we assumed that the power of burst is uniformly distributed over a frequency range upto 2000 Hz. We find, by setting thresholds for different detectors, that a network of power-recycled LIGOs and dual-recycled GEO and AIGO can increase the volume of the sky covered by only power-recycled LIGO detectors by about 4.9 times for the observation of the burst sources of the same strength. The absolute range of observation will vary with the strength of the burst.

(b) We find that a coincidence experiment of power-recycled LIGO detectors and VIRGO and dual-recycled GEO and AIGO can increase the volume of the sky covered by 3.2 times as compared with only power-recycled LIGO detectors and by 1.7 times as compared with the power-recycled LIGO-VIRGO network. This is of course far less than the range that can be covered by only LIGOs or the LIGO-VIRGO network with dual recycling operation, which they may implement in the later stage of their 'initial' interferometers but the accuracy in the determination of direction, distance and other source parameters will be much better in a coincidence experiment in which other detectors and especially AIGO can take part.

We suggest further investigations which need to be carried out on various issues related to this paper. As discussed in item (iv) above, although the actual number of filters may vary for different detectors, we made a conservative estimate of the number of filters to calculate the threshold levels. A detailed analysis, however, is in order taking into account several filter banks corresponding to different detectors. Secondly, the phase information can be used along with the time-delay information to decide on coincident detection. For this purpose the orientations of the detectors will have to be taken into account. As discussed in section IV B, it is also important to carry out a detailed investigation for the determination of the direction of the binary and thus also the window size using time-delays in the *time of coalescence* (instead of *time of arrival*) between different detectors (also see Ref. [44]). On similar lines as above, we could also treat other sources which have different power spectra. An important source that may be mentioned in this connection is the stochastic gravitational radiation. An analysis applying the results of the detailed investigations carried out by Christensen [45] and Flanagan [46] to the planned interferometers may come to be useful for the evaluation of the sensitivities of the networks for the detection of the stochastic radiation.

ACKNOWLEDGMENTS

We would like to specially thank J. Sandeman for suggesting to us this problem and D. Shoemaker for clarifying various points and for giving valuable comments on a preliminary version of this manuscript. It is also our pleasure to thank D. Blair, M. Fujimoto, D.E. McClelland, M. Taniwaki, J.-Y. Vinet and W. Winkler for clarifying some important points and supplying various information and R. Balasubramanium, S.D. Mohanty and B.S. Sathyaprakash for useful discussions.

---

[1] J. Weber, Phys. Rev., **117**, 306 (1960)

[2] K.S. Thorne, in *300 Years of Gravitation*, eds. S. hawking and W. Israel (Cambridge Univ. Press, Cambridge, 1987).

[3] K.S. Thorne, in the *Proceedings of the Snowmass '95 Summer Study on Particle and Nuclear Astrophysics and Cosmology*, eds. E.W. Kolb and R. Peccei (World Scientific, Singapore, 1995); K.S. Thorne, in *Proc. of IAU Symposium 165, Compact Stars in Binaries*, eds. J. van Paradijs, E. van den Heuvel, E. Kuulkers (Kluwer Academic Publishers, Dordrecht, The Netherlands, 1995)

[4] A. Abramovici, W.E. Althouse, R.W.P. Drever, Y. Gürsel, S. Kawamura, F.J. Raab, D. Shoemaker, L. Sievers, R.W. Spero, K.S. Thorne, R.E. Vogt, R. Weiss, S.E. Whitcomb, and M.E. Zucker, Science, **256**, 325 (1992).

[5] A. Giazotto *et al*, *The VIRGO project* (INFN, 1989); *VIRGO: Final conceptual design* (1992).

[6] J. Hough *et al*,*Proposal for a Joint German-British Interferometric Gravitational Wave Detector* (1989).
[7] R. Narayan, T. Piran, and A. Shemi, Astrophy. J. **379**, L17 (1991); E.S. Phinney, *ibid.* **380**, L17 (1992).
[8] A. Krolak, in *Gravitational Wave Data Analysis*, ed. B.F. Schutz (Kluwer, Dordrecht, 1989) pp. 59-69; S.V. Dhurandhar, A. Krolak, B. Schutz and J. Watkins, 'Filtering the gravitational Wave Signal of a Coalescing Binary', report (unpublished); L.S. Finn, Phys. Rev. D, **46**, 5236(1992)
[9] B.S. Sathyaprakash and S.V. Dhurandhar, Phys. Rev. D **44**, 3819 (1991)
[10] S.V. Dhurandhar and B.S. Sathyaprakash, Phys. Rev. D **49**, 1707 (1994)
[11] L.S. Finn and D.F. Chernoff, Phys. Rev. D **47**, 2198 (1993)
[12] A. Krolak, J.A. Lobo, B.J. Meers, Phys. Rev. D **48**, 3451 (1993)
[13] *Errors in a few equations given in Ref. [12] have been corrected in* A. Krolak, *unpublished note* (1994).
[14] B.F. Schutz, in *Gravitational Collapse and Relativity*, eds. H. Sato and T. Nakamura (World Scientific, Singapore, 1986), pp.350-458.
[15] B.F. Schutz, Nature, **323**, 310 (1986),
[16] B.F. Schutz, Cl. Qu. Grav., **6**, 1761 (1989),
[17] A. Krolak and B.F. Schutz, Gen. Rel. Grav., **19**, 1163 (1987).
[18] S.V. Dhurandhar and M. Tinto, Mon. Not. R. Astron. Soc., **234**, 663 (1988); M. Tinto and S.V. Dhurandhar, Mon. Not. R. Astron. Soc., **236**, 621 (1989)
[19] Y. Gürsel and M. Tinto, Phys. Rev D **40**, 3884 (1989).
[20] P. Jaranowski and A. Krolak, Phys. Rev. D **49**, 1723 (1994).
[21] S. Bourzeix, G. Boursin, B. Linet, Phys. Lett. A **151**, 371 (1990).
[22] C. Cutler and E. Flanagan, Phys. Rev. D **49**, 2658 (1994)
[23] D. Marković, Phys. rev. D **48**, 4738 (1993)
[24] B.F. Schutz (1989) *Data analysis requirements of networks of detectors* in *Gravitational wave data analysis* Ed. B.F. Schutz (Kluwer Academic Publishers, Dordrecht, The Netherlands, 1989) p. 315.
[25] J. Sandeman and D.E. McClelland, *private communication*.
[26] W. Winkler, in: The detection of gravitational waves, ed. D.G. Blair (Cambridge University Press, Cambridge, 1991);
[27] R.W.P. Drever, in: The detection of gravitational waves, ed. D.G. Blair (Cambridge University Press, Cambridge, 1991);
[28] R.W.P. Drever, in: Gravitational Radiation, ed. N. Deruelle and T. Piran (North-Holland, Amsterdam, 1983); P.Fritschel, D. Shoemaker and R. Weiss, Ap. Optics, **31**, 1412 (1992).
[29] J.-Y. Vinet, B.J. Meers, C.N. Man, A. Brillet, Phys. Rev., D **38**, 433 (1988); A. Brillet, J. Gea-Banacloche, G. Leuches, C.N. Man, J.-Y. Vinet, in: The detection of gravitational waves, ed. D.G. Blair (Cambridge University Press, Cambridge, 1991)
[30] J.-Y. Vinet, B.J. Meers, C.N. Man, A. Brillet, Phys. Rev., D **38**, 433 (1988); A. Giazotto, Phys. Rep., **182**, 365 (1989).
[31] B.J. Meers, Phys. Rev., D **38**, 2317 (1988); *ibid* Phys. Lett., A **142**, 465 (1989); K.A. Strain and B.J. Meers, Phys. Rev. Lett., **66**, 1391 (1991).
[32] P.R. Saulson, Phys. Rev., D **42**, 2437, (1990)
[33] A. Gillespie and F. Raab, Phys. Lett., A **178**, 357 (1993).
[34] A. Gillespie and F. Raab, Phys. Rev., D **52**, 577 (1995).
[35] R. Weiss, Quart. Prog. Rep. Res. Lab. Electronics, MIT **105**, 54 (1972); C.N. Man, D. Shoemaker, M. Pham Tu, D. Dewey, Phys. Lett., A **148**, 8 (1990).
[36] P.R. Saulson, Phys. Rev., D **30**, 732 (1984)
[37] J.-Y. Vinet, *private communication*,
[38] W. Winkler, *private communication*,
[39] M. Fujimoto, *private communication*,
[40] However, the final choice of this value will crucially depend on the mirror losses and the issue is not settled yet (D.H. Shoemaker, *private communication*).
[41] We may note here that the conclusion drawn by Krolak, Lobo and Meers [12] that the narrow-band dual recycling with a bandwidth of 6Hz around 100Hz is better than standard recycling for the observation of the inspiral waveform from binary systems is actually not valid when thermal noise is also taken into account, which they completely neglected. Our numerical calculation shows that actually the SNR for initial LIGO reduces by about 39% as compared to the power recycling case.
[42] M. Tinto and B.F. Schutz, Mon. Not. R. Astron. Soc., **224**, 131 (1987); M. Tinto, *ibid*, **226**, 829 (1987); M. Tinto, in *Gravitational Wave Data Analysis*, ed. B.F. Schutz (Kluwer, Dordrecht, 1989) p. 299.
[43] S. V. Dhurandhar and B.F. Schutz, Phys. Rev. D **50**, 2390 (1994)
[44] R. Balasubramanium, B.S. Sathyaprakash and S.V. Dhurandhar, *Gravitational waves from coalescing binaries : Detection strategies and Monte Carlo simulation for parameter estimation submitted for publication*.
[45] N. Christensen, Phys. Rev., D **46**, 5250 (1992).
[46] E.E. Flanagan, Phys. Rev., D **48**, 2389 (1993).

FIG. 1. The geometry of four detectors. Only solid lines and curves represent those in the plane of the paper. D_1 - the reference detector; D_2, D_3 - actual positions of detectors 2 and 3; θ, ϕ - direction of the source, S.

FIG. 2. V - VIRGO, H - LIGO at Hanford, L - LIGO at Livingston. The optimum window area in the shape of an ellipse for the HLV network. The maximum window size is the square area enclosed by the dashed lines.

FIG. 3. V - VIRGO, H - LIGO at Hanford, L - LIGO at Livingston. The time-delay between V and L, n_3 as a function of the angle ϕ of the direction of source for a fixed value (=15.) of the time delay, n_2 between V and H.

FIG. 4. The ellipsoidal surface for the time-delay, n_4 of the AHVL network. A - AIGO, V - VIRGO, H - LIGO at Hanford, L - LIGO at Livingston.

TABLE I. Description of the site and configuration of the planned detectors. The letter written in the second column represents the corresponding detector throughout our analysis. The orientation refers to the angle made by the bisector of the arms with the local south $\rightarrow$ north direction measured in anticlockwise convention. DL and FP in the 4th column refers to delay lines and Fabry-Perot cavities respectively, which are incorporated in the arms. The recycling configuration indicated in the fifth column is for the initial stages of the interferometers. All these detectors will have provision for incorporating dual recycling at later stages. The minimum length of the proposed AIGO detector has been set to be 500m, however, this may change, but not much, depending on the budget available.

Detector	Denoted by	Length	Arms	Recycling	Latitude	Longitude	Orientation
LIGO, Hanford, Washington	H4	4000m	FP	Power	$46^0 27' 18.5'' \mathrm{N}$	$119^0 24' 27.1'' \mathrm{W}$	81.8^0
LIGO, Hanford, Washington	H2	2000m	FP	Power	$46^0 27' 18.5'' \mathrm{N}$	$119^0 24' 27.1'' \mathrm{W}$	81.8^0
LIGO, Livingston, Lousiana	L	4000m	FP	Power	$30^0 33' 46.0'' \mathrm{N}$	$90^0 46' 27.3'' \mathrm{W}$	153^0
VIRGO, Pisa, Italy	V	3000m	FP	Power	$43.3^0 \mathrm{N}$	$10.1^0 \mathrm{E}$	26.5^0
GEO, Hannover, Germany	G	600m	DL(3 bounces)	Dual	$52^0 14.8' \mathrm{N}$	$9^0 49.3' \mathrm{E}$	339.25^0
AIGO, Perth, Australia	A	$\sim$ 500m	DL(3 bounces)	Dual	$31.04^0 \mathrm{S}$	$115.49^0 \mathrm{E}$	*not decided*
TAMA, Mitaka, Japan	T	300m	FP	Power	$35^0 40' 25'' \mathrm{N}$	$139^0 32' 15'' \mathrm{E}$	225^0

TABLE II. Values of the parameters used in the calculation of the relative signal to noise ratio of the detectors. In most of the cases, these have been obtained by personal communication with people involved in designing the planned detectors. Some of these are quoted as *conservative estimates*, while others are quoted to be *hopefully achievable ones*. Values marked with (*) are assumed by us. The value of R_1 for H2 has been chosen such that its cavity finesse becomes approximately twice that of H4. It should be noted that the TAMA (300m) interferometer has been designed to work as a prototype in its initial stage.

Quantities	L,H4	H2	V	G	A	T
End mass, m(Kg)	10	10	42	16	16	1
Suspension quality, Q_0	10^7	10^7	3×10^5	5×10^7	5×10^7	10^5
End mass fundamental mode, $f_{\rm int}$(KHz)	23	23	5.7	20^*	20^*	30
End mass quality, $Q_{\rm int}$	10^5	10^5	10^6	5×10^6	5×10^6	5×10^5
Laser power, ηI_0(watts)	5	5	10	5	5	3
Laser wavelength, $\lambda(\mu$meter)	0.514	0.514	1.06	1.06	1.06	1.06
Mirror losses, $A^2(\times 10^{-6})$	50.	50.	2.	20.	20.	10.
Input mirror reflectivily of cavity,R_1	0.97	0.985^*	0.85	-	-	0.988

TABLE III. Relative SNRs of the detectors, $\zeta^{\rm J}_{\rm cb}$ and $\zeta^{\rm J}_{\rm bur}$ as normalised with respect to that of full length LIGO using power recycling *for the same kind of source* . A - AIGO, H4 - 4000m LIGO at Hanford, H2 - 2000m LIGO at Hanford, L - LIGO at Livingston, G - GEO, V - VIRGO, T - TAMA. The dual recycling parameters are, in all cases, chosen to be those for a bandwidth of 300Hz around 250Hz as will be used in GEO. It should be noted that for different detectors, maximum gain may be obtained for some different values for bandwidth and central frequency. †Although the dual recycling values for LIGO, VIRGO and TAMA have been calculated, but they do not have any plan to implement this at the initial stage of their interferometers. It should also be noted that the TAMA (300m) interferometer has been designed to work as a prototype in its initial stage.

Detector	$\zeta^{\rm J}_{\rm cb}$(Power)	$\zeta^{\rm J}_{\rm cb}$(Dual)	$\zeta^{\rm J}_{\rm bur}$(Power)	$\zeta^{\rm J}_{\rm bur}$(Dual)
L, H4	1.0	$2.78^{\dagger}$	1.0	$6.03^{\dagger}$
H2	0.58	$1.38^{\dagger}$	0.66	$3.01^{\dagger}$
V	1.25	$1.93^{\dagger}$	4.33	$9.36^{\dagger}$
G	0.13	0.95	0.15	1.82
A	0.11	0.79	0.13	1.51
T	0.028	$0.034^{\dagger}$	0.168	$0.230^{\dagger}$

TABLE IV. Maximum time delays, N_2 between two detectors. A - AIGO, H - LIGO at Hanford, L - LIGO at Livingston, G - GEO, V - VIRGO, T - TAMA.

Detectors	Maximum delay	Detectors	Maximum delay	Detectors	Maximum delay
HL	10.0	HV	27.2	LV	26.3
HG	25.0	LG	25.0	VG	3.3
HA	39.2	LA	41.6	VA	37.0
GA	37.3	HT	14.6	LT	22.0
VT	21.4	AT	35.2	GT	18.5

TABLE V. Window sizes for 3-detector networks. A - AIGO, H - LIGO at Hanford, L - LIGO at Livingston, G - GEO, V - VIRGO, T - TAMA.

Network	Optimized area	Network	Optimized area
VHL	822.2	GHL	769.5
AHL	1222.6	LVG	243.9
ALV	3012.8	HVG	201.3
AHV	3031.3	ALG	2894.9
AHG	2831.0	AVG	383.2
THL	372.0	THV	975.6
THG	841.4	TGV	98.4
TLG	1238.9	TLV	1425.9
ATL	2432.8	ATV	2309.7
ATG	2023.9	ATH	1609.1

TABLE VI. Threshold to be set for different detectors for coincident observation of millisecond burst sources. A - AIGO, H4 - 4000m LIGO at Hanford, H2 - 2000m LIGO at Hanford, L - LIGO at Livingston, G - GEO, V - VIRGO. H - represents both detectors at Hanford together. For networks with detectors at more than three sites, the first detector represents the reference detector, whereas the first three detectors represent the reference 3-detector network, on the basis of which we calculated the window size (*see text*). The superscripts (^{p}) and (^{d}) represent the power and dual recycling modes of opration respectively.

Network of detectors	H4	H2	L	V	G	A
$H4^pH2^p$	5.37	3.54	-	-	-	-
$H4^pH2^d$	2.05	6.17	-	-	-	-
$H4^pL^p$or $H4^dL^d$	4.85	-	4.85	-	-	-
$H4^pH2^pL^p$	4.30	2.84	4.30	-	-	-
$G^dH4^pH2^pL^p$	2.95	1.95	2.95	-	5.37	-
$G^dH4^pL^p$	3.13	-	3.13	-	5.70	-
$A^dH4^pH2^pL^p$	3.28	2.16	3.28	-	-	4.95
$A^dH4^pL^p$	3.50	-	3.50	-	-	5.28
$A^dH4^pH2^pG^dL^p$	2.54	1.67	2.54	-	4.62	3.83
$A^dH4^pG^dL^p$	2.65	-	2.65	-	4.82	4.00
A^dG^d	-	-	-	-	5.42	4.50
$H4^dH2^dL^d$	4.47	2.23	4.47	-	-	-
$V^pH4^dH2^dL^d$	4.24	2.12	4.24	3.04	-	-
$V^dH4^dH2^dL^d$	3.27	1.64	3.27	5.09	-	-

TABLE VII. Thresholds to be set for different detectors for coincident observation of coalescing compact binary sources. A - AIGO, H4 - 4000m LIGO at Hanford, H2 - 2000m LIGO at Hanford, L - LIGO at Livingston, G - GEO, V - VIRGO. H - represents both detectors at Hanford together. For networks with detectors at more than three sites, the first detector represents the reference detector, whereas the first three detectors represent the reference 3-detector network, on the basis of which we calculated the window size (*see text*). The superscripts (^{p}) and (^{d}) represent the power and dual recycling modes of operation respectively.

Network of detectors	H4	H2	L	V	G	A
$H4^pH2^p$	6.45	3.74	-	-	-	-
$H4^pH2^d$	4.37	6.03	-	-	-	-
$H4^pL^p$or $H4^dL^d$	5.53	-	5.53	-	-	-
$H4^pH2^pL^p$	5.02	2.91	5.02	-	-	-
$H4^pH2^dL^p$	3.87	5.34	3.87	-	-	-
$V^pH4^pH2^pL^p$	4.04	2.34	4.04	5.05	-	-
$V^pH4^pH2^dL^p$	3.40	4.70	3.40	4.25	-	-
$V^pH4^pL^p$	4.30	-	4.30	5.37	-	-
$G^dH4^pH2^pL^p$	4.43	2.57	4.43	-	4.21	-
$G^dH4^pH2^dL^p$	3.63	5.00	3.63	-	3.45	-
$G^dH4^pL^p$	4.76	-	4.76	-	4.52	-
$A^dH4^pH2^pL^p$	4.66	2.70	4.66	-	-	3.68
$A^dH4^pH2^dL^p$	3.77	5.20	3.77	-	-	2.98
$A^dH4^pL^p$	5.02	-	5.02	-	-	3.96
$V^pH4^pH2^pL^pG^d$	3.62	2.10	3.62	4.52	3.44	-
$V^pH4^pH2^dL^pG^d$	3.14	4.33	3.14	3.91	2.98	-
$V^pH4^pL^pG^d$	3.80	-	3.80	4.75	3.62	-
$A^dV^pH4^pH2^pL^p$	3.80	2.20	3.80	4.75	-	3.00
$A^dV^pH4^pH2^dL^p$	3.27	4.51	3.27	4.09	-	2.58
$A^dV^pH4^pL^p$	4.01	-	4.01	5.01	-	3.17
$A^dH4^pH2^pG^dL^p$	4.10	2.38	4.1 0	-	3.89	3.24
$A^dH4^pH2^dG^dL^p$	3.46	4.77	3.46	-	3.28	2.73
$A^dH4^pG^dL^p$	4.36	-	4.36	-	4.14	3.44
$A^dV^pH4^pH2^pL^pG^d$	3.42	1.98	3.42	4.27	3.25	2.70
$A^dV^pH4^pH2^dL^pG^d$	3.00	4.14	3.00	3.75	2.85	2.37
$A^dV^pH4^pL^pG^d$	3.57	-	3.57	4.46	3.39	2.82
A^dG^d	-	-	-	-	6.14	5.10
$H4^dH2^dL^d$	5.13	2.55	5.13	-	-	-
$V^dH4^dH2^dL^d$	4.83	2.40	4.83	3.35	-	-
$A^dV^pH4^pH2^pL^pG^d$	4.69	2.33	4.69	3.26	1.60	1.33

TABLE VIII. The range of observation and the source rate of coalescing binaries for some interesting networks of the initial detectors coming up at the beginning of the next century. These values correspond to binaries of chirp mass $1.2M_{\odot}$. The calculation of the source rates is based a conservative estimate of the expectation rate $\{8 \times 10^{-8}\}$ Mpc^{-3} yr^{-1} and a maximum limit of $\{6 \times 10^{-5}\}$ Mpc^{-3} yr^{-1}. For other values of chirp mass and source rate, see the text. † Although the last entry of this table corresponds to a coincident experiment in which all detectors are operated in dual recycling mode, actually, such an experiment would not be a meaningful one because the thresholds for GEO and AIGO (with their present design parameters) are to be set at very low values compared to LIGOs and VIRGO (*for more explanation see the text*).

Network of detectors	Range, $\mathcal{R}_{90\%}$ (Mpc)	Source rate (yr^{-1}) (conservative estimate)	Source rate (yr^{-1}) (maximum limit)
L^por $H4^p$alone	37.67	0.004	3.19
$H4^pH2^pL^p$	57.41	0.015	11.30
$H4^pH2^dL^p$	74.47	0.033	24.67
$V^pH4^pH2^pL^p$	68.95	0.026	19.58
$V^pH4^pH2^pL^pG^d$	77.48	0.037	27.78
$A^dV^pH4^pH2^pL^p$	73.71	0.032	23.92
$A^dV^pH4^pH2^pL^pG^d$	82.35	0.045	33.35
$A^dV^pH4^pH2^dL^pG^d$	94.19	0.067	49.91
L^dor $H4^d$alone	104.74	0.092	68.63
$H4^dL^d$	144.89	0.242	181.68
$H4^dH2^dL^d$	156.19	0.303	227.58
$V^dH4^dH2^dL^d$	165.89	0.364	272.68
$A^dV^dH4^dH2^dL^dG^{d\dagger}$	170.84	0.397	297.83

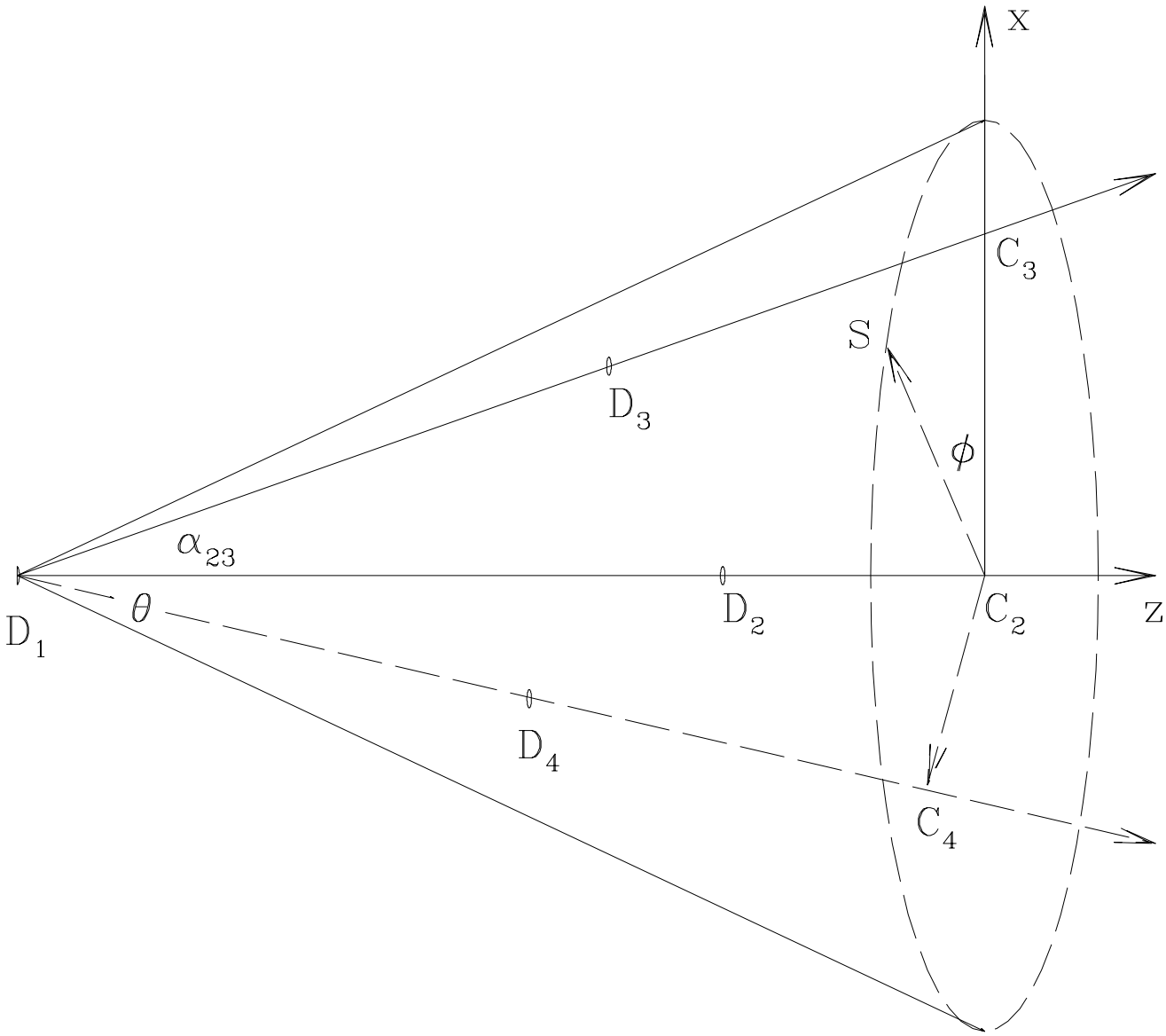

FIG. 1

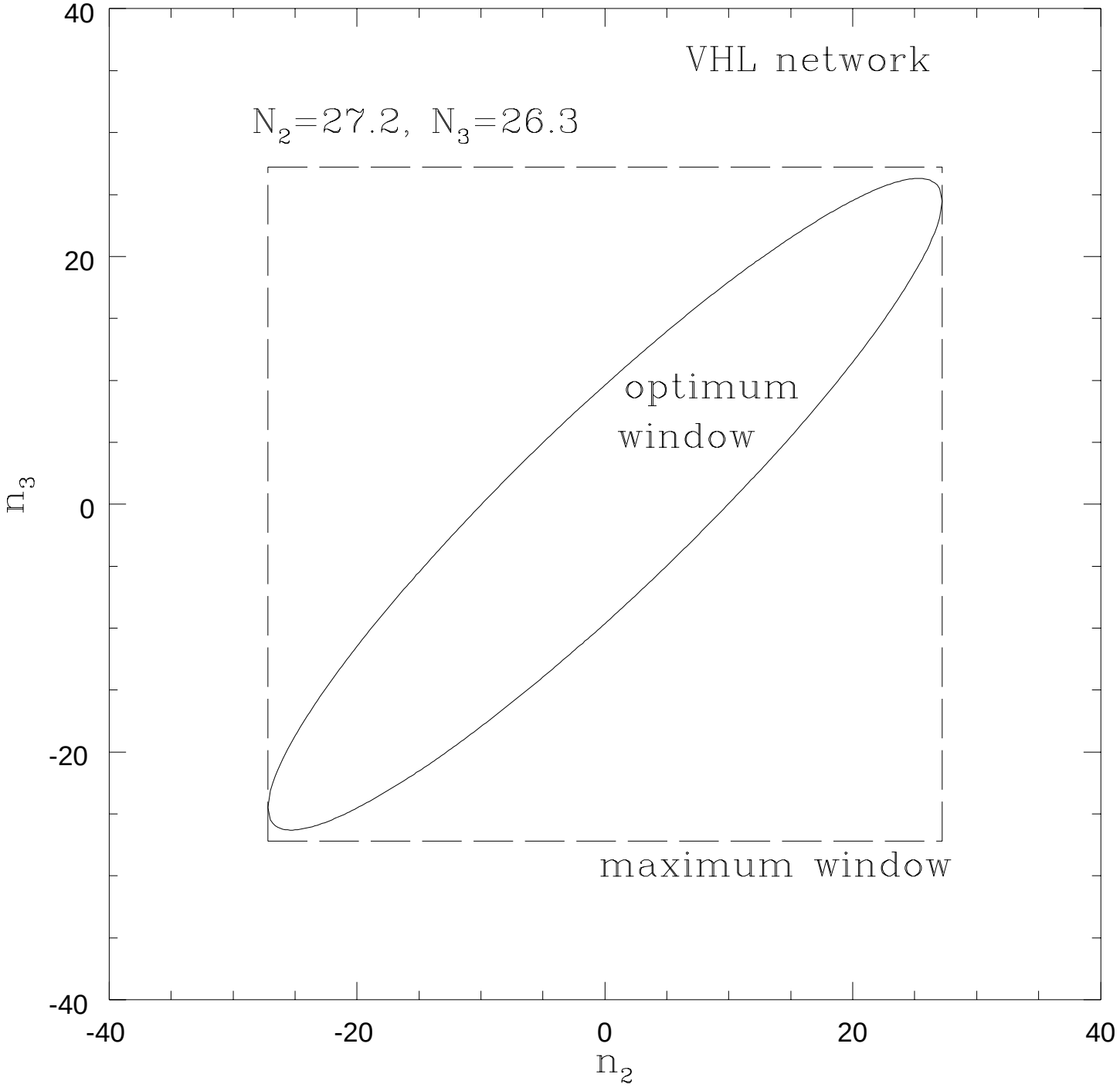
VHL network
N_2=27.2, N_3=26.3
optimum
window
maximum window
40
20
0
-20
-40
-40
-20
0
20
40
n_3
n_2

FIG.2

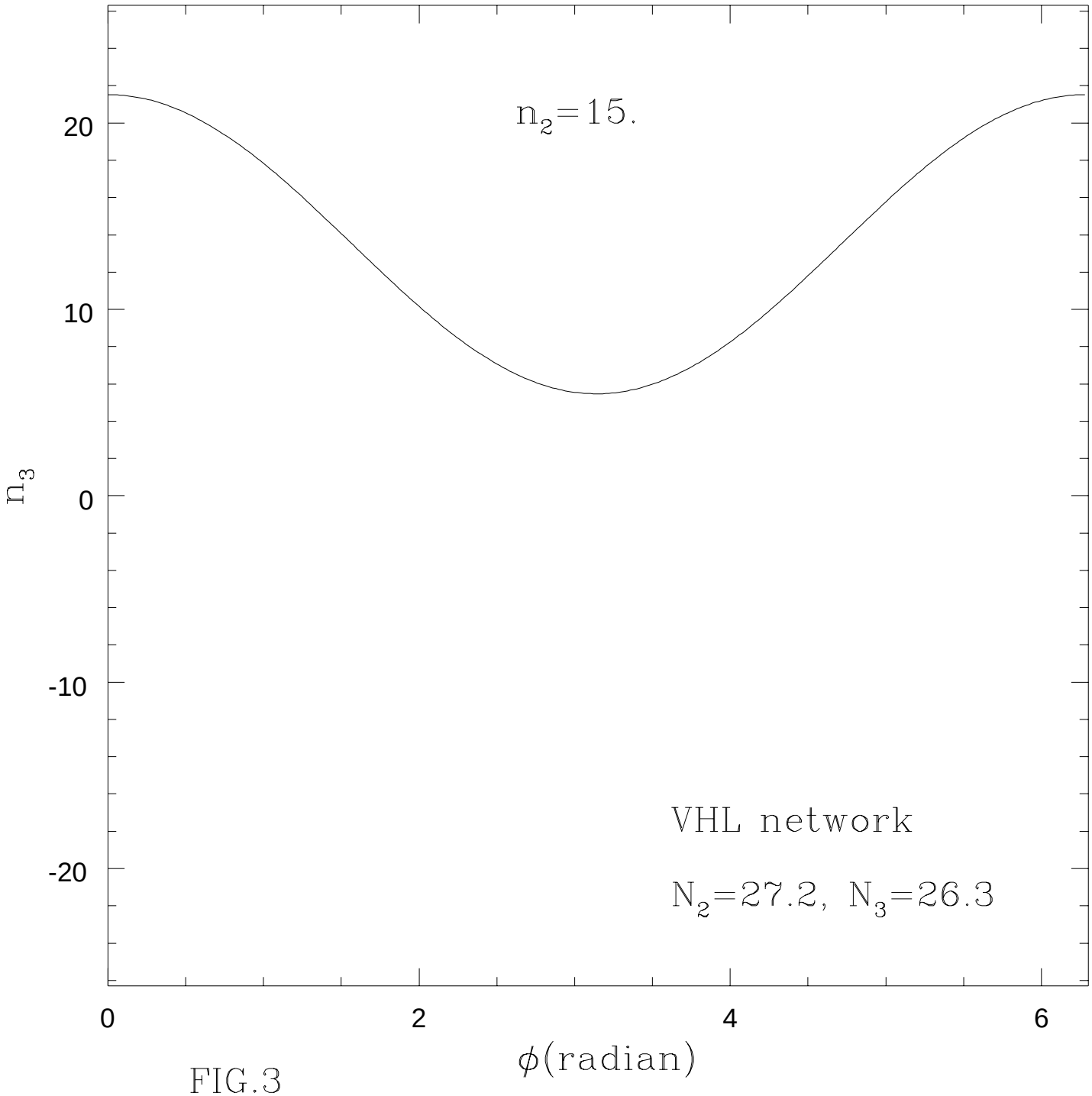

FIG.3

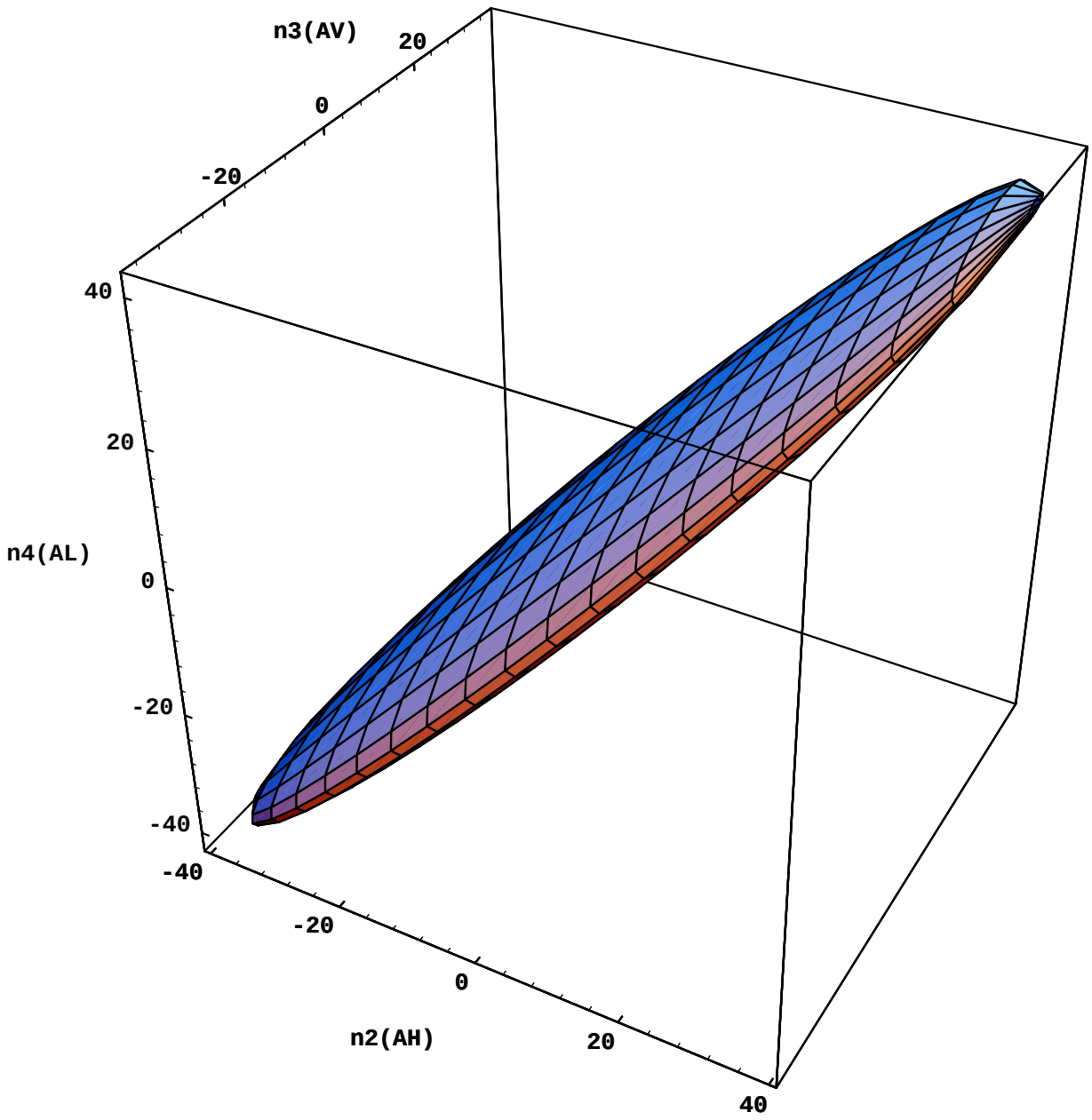
n3(AV)
20
0
-20
40
20
n4(AL)
0
-20
-40
-40
-20
0
n2(AH)
20
40